

1 **Entropy of a bacterial stress response is a generalizable predictor for fitness and antibiotic
2 sensitivity.**

3

4

5

6 Zeyu Zhu^{1†}, Defne Surujon^{1†}, Juan C. Ortiz-Marquez¹, Stephen J. Wood¹, Wenwen Huo³, Ralph R.
7 Isberg³, José Bento², and Tim van Opijnen^{1*}

8

9

10

11 ¹Biology Department, Boston College, Chestnut Hill, MA, USA

12 ² Computer Science Department, Boston College, Chestnut Hill, MA, USA

13 ³ Department of Molecular Biology and Microbiology, Tufts University School of Medicine,
14 Boston, MA, USA

15

16

17

18 [†] Equal contribution

19 * Corresponding author

20

21

22

23

24

25 **Keywords:**

26 RNA-Seq

27 Tn-Seq

28 antibiotic resistance

29 systems biology

30 machine learning

31 data integration

32 predictive modeling

33 **Abstract**

34 Genes implicated in bacterial stress responses have been used to construct models that infer the growth
35 outcome of a bacterium in the presence of antibiotics with the objective to develop novel diagnostic
36 methods in the clinic. Current models are trained on data specific to a species or type of stress, making
37 them potentially limited in their application. It is unclear if a generalizable response-signature exists that
38 can predict bacterial fitness independent of strain, species or type of stress. Here we present a substantial
39 RNA-Seq and experimental evolution dataset for 9 strains and species, under multiple antibiotic and non-
40 antibiotic stress conditions. We show that gene panel-based models can accurately predict antibiotic
41 mechanism of action, as well as the fitness outcome of *Streptococcus pneumoniae* in the presence of
42 antibiotics or under nutrient depletion. However, these models quickly become species-specific as gene
43 homology is limited. Instead, we define a new concept, transcriptomic entropy, which we use to quantify
44 the amount of transcriptional disruption that occurs in a bacterium when responding to the environment.
45 With entropy at the center, we train a suite of predictive (machine learning) models enabling generalizable
46 fitness and antibiotic sensitivity predictions. These entropy-based models that predict bacterial fitness are
47 validated for 7 Gram-positive and -negative species under antibiotic and non-antibiotic conditions
48 indicating that transcriptomic entropy can be used as a generalizable stress signature. Moreover, rather
49 than being a binary indicator of fitness, an entropy-based model was developed and validated to predict
50 the minimum inhibitory concentration of an antibiotic. Lastly, we show that the inclusion of a varied-set
51 of multi-omics features of a bacterial stress response further enhances fitness predictions by reducing
52 ambiguity. By demonstrating the feasibility of generalizable predictions of bacterial fitness, this work
53 establishes the fundamentals for potentially new approaches in infectious disease diagnostics, including
54 antibiotic susceptibility testing.

55 **Significance statement**

56 Accurate predictions of bacterial fitness outcome could potentially have clinical diagnostic value, such as
57 predicting optimum antibiotic choice and dosage for treating infectious diseases. Existing models of
58 fitness predictions rely mainly on gene panel approaches, which may be species- and stress-specific due
59 to a lack of gene and response conservation. In order to overcome this limitation, we generated a
60 substantial experimental dataset and identified entropy as a universal stress response signature that
61 quantifies the level of transcriptional disruption that is indicative of fitness outcome under a stressful
62 condition. We present and validate for Gram-positive and negative species a suite of entropy-based models
63 that enable accurate predictions of fitness outcome and the level of antibiotic sensitivity in a species and
64 stress-type independent manner.

65 **Introduction**

66 It is generally assumed that in order to overcome a stress, bacteria activate a response such as the stringent
67 response under nutrient deprivation (1) or the SOS response in the presence of DNA damage (2).
68 Measuring the activation of a specific response, or genes associated with this response, can thereby
69 function as an indicator of what type of stress is occurring in a bacterium. For instance, *lexA*, encoding a
70 master regulator of the SOS response in *Escherichia coli* and *Salmonella* (3, 4) is upregulated in response
71 to fluoroquinolones, indicative of the DNA damage resulting from this class of antibiotics (4). Moreover,
72 genes implicated in a stress response can help construct statistical models for predicting growth outcomes
73 under that stress. For instance, gene panels have been assembled from transcriptomic data to predict
74 whether *E. coli* can successfully grow in the presence of antibiotics such as ciprofloxacin (5-7).

75

76 While a defined stress-response or a gene-panel can be valuable in identifying the type or sensitivity to a
77 stress, there are several complications that make one-to-one implementation across strains, species or
78 environments difficult. For instance, responses such as the stringent or SOS response are only well defined
79 in a small number of species, genes in a gene-panel may not be conserved across strains or species, and
80 responses are not necessarily regulated in the same manner in different strains or species (8, 9). This lack
81 of well-characterized and/or conserved responses limits the potential generalizability of existing models
82 that attempt to predict stress sensitivity across strains and species. Therefore, identification of a universal
83 stress response signature would allow for the development of generalizable predictive models that work
84 for any species under any condition. There is not, however, a generally agreed upon stress response
85 signature.

86

87 We previously showed that a stress response can be captured on at least two organizational levels; with
88 RNA-Seq genome-wide transcriptional changes upon an environmental perturbation can be described,
89 while transposon-insertion sequencing (Tn-Seq) characterizes the phenotypic importance of a gene, i.e. a
90 gene's contribution to fitness in a specific environment, on a genome-wide scale (16-21). Direct
91 comparisons of data obtained from these approaches revealed that genes that change in transcription are
92 poor indicators of what matters phenotypically (16). In other words, phenotypically important and
93 transcriptionally important genes rarely overlap (16). However, when integrated into a network,
94 coordinated patterns between these data-sets surface when the organism is challenged with an
95 evolutionarily familiar stress (i.e. one that has been experienced for many generations), while the response

96 becomes less coordinated when the bacterium is challenged with and responds to a relatively new stress,
97 for instance antibiotics (16). This suggests that a stress signature may exist that is indicative of the degree
98 to which a bacterium is adapted to a specific stress and is able to overcome the challenge. To determine
99 whether such a signature exists and whether it is universal we generated and mined a substantial
100 experimental dataset for the bacterial pathogen *Streptococcus pneumoniae*. We first demonstrate that both
101 an antibiotic's MOA and the bacterium's fitness under antibiotic or nutrient pressure can be predicted by
102 expression profiles from two distinct small gene-panels. However, these panels are limited to strains and
103 species sharing high sequence and response homology. Instead, we develop the concept of entropy and
104 build a suite of predictive models that accurately predict a bacterium's fitness outcome under various
105 nutrient, antibiotic and transcriptional perturbation conditions. Moreover, entropy is quantitatively
106 correlated with the level of antibiotic sensitivity, enabling MIC predictions. We show the universality of
107 entropy by validation experiments with 7 Gram-negative and -positive pathogenic species. We further
108 demonstrate that entropy-based models can be improved in accuracy when different data-types are
109 combined into a Support Vector Machine. Overall, we develop a large new experimental dataset, a novel
110 species-independent stress-response concept and a suite of predictive models that accommodate different
111 amounts and types of data to enable generalizable fitness predictions and antibiotic sensitivity.
112
113

114 **Results**

115 **Antibiotic transcriptional responses are distinguishable based on mechanisms of action.**

116 To determine if the transcriptional responses to antibiotics were dependent on their mechanisms of action,
117 the TIGR4 (T4) and Taiwan-19F (19F) strains of *Streptococcus pneumoniae* were grown in the presence
118 or absence of 1x the minimum inhibitory concentration (MIC) of 9 antibiotics representing 4 mechanisms
119 of action (MOA's). These include cell wall synthesis inhibitors (CWSI), DNA synthesis inhibitors (DSI),
120 protein synthesis inhibitors (PSI) and RNA synthesis inhibitors ((RSI); **Figure 1A**, Supplemental Tables
121 1, 6). Each strain was exposed to each antibiotic for 2 to 4 hours and cells were harvested for RNA-Seq at
122 various time points after antibiotic exposure. Previous models have predicted bacterial fitness of
123 *Escherichia coli* exposed to specific stressful conditions by relying on differential expression of selected
124 small gene sets (5-7). Before we set out to determine whether a generalizable feature can predict fitness
125 across a variety of stress types, we first established if a small gene set can predict the MOA of an antibiotic
126 and/or fitness of *S. pneumoniae* (**Figure 1A**). Principal component analysis (PCA) was performed on the
127 complete differential transcription datasets, and this indicated that temporal transcriptional responses to
128 drugs within the same MOA tended to follow similar trajectories over time (**Figure 1B, C**).

129

130 To infer MOA's from the transcriptional profiles, a regularized logistic regression was used for unbiased
131 feature selection. Since, the number of genes available to use as features far exceeds the number of RNA-
132 Seq experiments this results in a high risk of overfitting, which can be overcome by strong regularization.
133 As previous gene-panel models have used up to 9 genes in any one panel (5, 6), we set the regularization
134 strength such that up to a total of 10 genes would be selected, with at least one gene for each MOA. This
135 reduced the data to a set of 8 genes (2 selected for CWSI, 3 for DSI, 2 for PSI and 1 for RSI) that maximally
136 separate the MOA's (**Figure 1D**, Supplemental Tables 2, 3). Notably, several genes in this panel and their
137 differential transcription patterns are functionally related to the antibiotics' MOA. First, up-regulation of
138 the repair DNA polymerase I (SP_0032) is predictive of a DSI which causes double stranded breaks by
139 trapping DNA topoisomerase IV and DNA gyrase. Second, increased transcription of RNA polymerase
140 subunit D (SP_1073) predicts a response to the transcription inhibitor rifampicin (RSI) and may also
141 represent a feedback response to rifampicin to maintain transcription levels. Third, the PSI kanamycin
142 drastically increases transcription of *clpP* (encoding a subunit of Clp protease) by 270-fold and 137-fold
143 in T4 and 19F, respectively. Aminoglycosides cause protein mistranslation, which leads to protein
144 aggregate formation that could be relieved by Clp protease (10). A similar response to PSI was observed

145 in *B. subtilis* (11), indicating that this may be diagnostic of a cellular response to remove mistranslated
146 proteins. Finally, in the presence of CWSI there is up-regulation of the two-component system CiaRH
147 (*ciaR* (SP_0798)), which has been associated with preventing lysis triggered by CWSIs in *S. pneumoniae*
148 (12, 13). In addition to these genes that are clearly connected to a specific MOA, the panel contains genes
149 with less clear connections with the MOA, i.e. SP_2107 (maltose metabolism), SP_2141 (glycosyl
150 hydrolase-like protein), SP_0021 (deoxyuridine 5'-triphosphate nucleotidohydrolase) and SP_2229 (Trp
151 tRNA synthetase) that allow the set to distinguish MOAs. The presence of such genes, along with well-
152 characterized genes relevant to the MOA confirms that the gene panel selection is unbiased and
153 independent of gene function annotations.

154

155 To enable MOA predictions from expression data without prior knowledge of the antibiotics used, the 8-
156 gene panel profiles were used to train a support vector machine (SVM) that classifies the MOA of the
157 antibiotic, which resulted in accurate prediction of MOAs (0.92) (**Figure 1E - Train**). The SVM was
158 validated using an independent transcriptional data-set collected from T4 and 19F treated with cefepime
159 (CEF), tetracycline (TET) and ciprofloxacin (CIP; **Figure 1E - Test**, Supplemental Table 1), resulting in
160 an accuracy of 0.75 (random chance results in an accuracy of 0.25). The lower accuracy in the test set
161 (compared to the training set) is mostly due to misclassification of ‘early’ exposure time points or
162 confusion of the model between the PSI and RSI MOA (Supplemental Notes), which can also be seen in
163 the close resemblance between the RSI and PSI PCA trajectories (**Figure 1B**). From a biological
164 perspective, this similarity is likely due to the closely related cellular functions blocked by the two MOAs
165 (i.e. transcription and translation).

166

167 **Low and high fitness outcomes after antibiotic exposure or nutrient deprivation of *S. pneumoniae*
168 can be represented by a single 10-gene signature.**

169 As T4 and 19F are susceptible to most antibiotics used, the transcriptional profiles in the presence of
170 antibiotics mostly represent cases of low fitness (**Figure 2A**, sensitive strain, 1xMIC_{WT}). Besides the
171 MOA-specific responses, we hypothesized that there may also be a single signature of low fitness
172 outcomes that can be extracted from the transcriptional profiles. In order to find patterns that differentiate
173 fitness outcomes (presence or absence of growth in a particular environment), we generated strains with
174 increased fitness in the presence of antibiotics through serial passaging wildtype T4 and 19F in the
175 presence of increasing amounts of antibiotics. Four independent populations for each strain were selected

176 on individual antibiotics to a point that they would grow at 1.5xMIC of the wildtype strain, albeit with a
177 small growth defect (Supplemental Figure 1A, B). To identify signatures of fitness, the wild type and
178 adapted clones were exposed for 2 to 4 hours to 1x and 1.5-2xMIC of the antibiotics used for adaptation,
179 followed by RNA-Seq at different time points after exposure (**Figure 2A**, Supplemental Figure 1A). In
180 parallel, RNA-Seq was performed on *S. pneumoniae* strains D39 and T4 in a chemically defined medium,
181 and media from which either uracil, Glycine or L-Valine was removed. This allowed for the identification
182 of a common stress signature that applies to nutrient deprivation as well, as these nutrients are essential
183 for D39 but not T4. Lastly, D39 was adapted to grow in the absence of each individual nutrient, after
184 which RNA-Seq was repeated for adapted clones (Supplemental Table 1 lists all 24 strains, 67 populations
185 and 6 species, and 267 RNA-Seq experiments; visualizable and explorable online at
186 <http://bioinformatics.bc.edu/shiny/ABX>).

187

188 To determine whether specific transcriptional differences exist that distinguish a strain that successfully
189 grows in a particular environment (high fitness) from one that does not (low fitness), the dataset was split
190 into stress-sensitive and stress-insensitive (e.g. adapted) groups. This approach identified three
191 transcriptional patterns. First, an unadapted, stress-sensitive strain tends to trigger a greater number of
192 transcriptional changes at 1xMIC or during nutrient deprivation compared to an adapted strain
193 (Supplemental Figure 2A-C). Second, in response to antibiotic or nutrient deprivation stress, the
194 magnitude of transcriptional changes in the stress-sensitive strains shows a broad distribution over time
195 compared to the adapted strains, indicating that there is extensive genome-wide transcriptional change in
196 sensitive strains (**Figure 2A, B**; Supplemental Figure 2D-F). Finally, stress-sensitive strains have a
197 significantly lower Kullback-Leibler divergence (KLD) relative to adapted strains, indicating higher
198 similarity of differentially expressed (DE) genes compared to the distribution of the entire genome. A
199 lower KLD therefore indicates a similar function distribution in DE genes and the genome, which can be
200 interpreted as a lack of functional enrichment in the differentially expressed genes (**Figure 2A, C**).
201

202 Logistic regression was used on the training part of the RNA-Seq dataset (231 experimental conditions;
203 Supplemental Table 1) to identify a gene panel that could accurately separate stress-sensitive from stress-
204 insensitive responses in a strain- and environment-independent manner. Similar to the selection of the
205 MOA-prediction gene panel, regularization was applied such that the number of genes used did not exceed
206 10. This resulted in a 10-gene-panel (Supplemental Tables 2, 3) that is able to separate and predict low

207 and high fitness outcomes with an accuracy of 0.91 for the training set (**Figure 3A**) and 0.83 for the
208 independent test set (**Figure 3B**, Supplemental Table 4; see Supplemental Notes for details on
209 misclassifications). These 10 genes showed similar DE patterns in low fitness outcomes in all the tested
210 strains and environments, and remained mostly unchanged in high fitness outcomes (**Figure 3C**). The
211 functions of these genes include cell division (*ftsZ*; SP_1666), metal ion transport (SP_1857 and
212 SP_1869), competence (SP_0955), cell surface protein (SP_2201), transcriptional regulation (SP_1856
213 and SP_1800), translation (SP_0929) and metabolism (SP_1478 and SP_0589). Unlike the MOA gene
214 panel, genes in the fitness gene panel are not obviously related to the antibiotics or depleted nutrients, but
215 may be pointing to a more general stress-response.

216

217 **Transcriptional responses can be captured by entropy, a generalizable feature for fitness
218 predictions.**

219 Although the gene panel-based fitness predictions show high accuracy for the tested conditions in *S.*
220 *pneumoniae*, it is unlikely that a small gene panel model is able to predict fitness outcomes for a wider
221 variety of conditions or for multiple species. Indeed the 10 *S. pneumoniae* genes that indicate fitness
222 outcomes are poorly conserved in *E. coli*, *Salmonella* Typhimurium and 3 ESKAPE species, including
223 *Acinetobacter baumannii*, *Klebsiella pneumoniae*, and *Staphylococcus aureus* (**Figure 3D**). Similarly,
224 only 3 out of 5 genes in a published *E. coli* ciprofloxacin sensitivity gene panel are present in all 6 species,
225 indicating that a gene panel approach is limited in its generalizability ((5); **Figure 3E**).
226

227 Our analysis indicates that in low-fitness cases, there is a corresponding disruption in transcriptional
228 regulation compared to a high-fitness scenario. To explore this idea, we leveraged the concept of entropy
229 to quantify the extent of transcriptomic disruption triggered by a stress. Using the information theory
230 definition of entropy, this concept captures the amount of chaos in a system, implemented here by
231 quantifying the variance in differential expression that occurs over time under stress conditions in a gene
232 or a collection of genes. (**Figure 2B**, Supplemental Figure 2). Our dataset contains 29 detailed RNA-Seq
233 time course experiments for which entropy was calculated initially by taking each gene in the system as
234 an independent entity (**Figure 4A**, Model 1). The average of the extent of transcriptional perturbation
235 across all genes in the genome was quantified by defining entropy as the average of the variance in
236 differential expression over time for all genes (Supplemental Methods, Equation 2; **Figure 4A**, Model 1).
237 To enable predictions, a model based on this single feature was trained by finding just one scalar number,

238 a threshold for entropy, to distinguish high fitness (below threshold) from low fitness (above threshold)
239 (**Figure 4B**, Supplemental Figure 3B). This model performs well, with only 1 false negative, i.e. a sample
240 with high fitness having an entropy value above the threshold (**Figure 4B**), but it assumes that each gene
241 behaves independently. This assumption does not capture biological complexity, as many genes co-vary
242 in expression, which can lead to over-estimating entropy if these dependencies are not accounted for.

243

244 To correct for co-variances in expression and their potentially confounding effects, we consider a gene
245 co-expression network, where, if the transcription of two genes have high co-variance, these genes are
246 connected. While the underlying co-transcriptional network is unknown for *S. pneumoniae*, it can be
247 inferred using the available temporal RNA-Seq data by computing the inverse of the co-variance matrix
248 of transcriptional changes among all gene pairs. This approach yielded a complete network, in which all
249 possible links between gene pairs were present and weighted by the co-variance values. This is equivalent
250 to considering the differential expression of all genes from all time points to be a multivariate Gaussian
251 distribution with as many dimensions as there are genes (Supplemental Methods; Equation 3). We
252 computed entropy for this multivariate distribution and set the appropriate threshold for separating high
253 and low fitness (**Figure 4A**, Model 2). All samples with higher entropy than the threshold were instances
254 of low fitness (**Figure 4C**, Supplemental Figure 3C), but 5 low fitness samples appeared to have low
255 entropy as well (false positives). This result is likely a consequence of considering ‘raw’ co-variance
256 values, which leads to the appearance of spurious links in the network that do not reflect real links between
257 genes. Therefore, Model 2 may overestimate the number of links between genes. To correct for such
258 spurious links, regularization was applied on the inverse of the co-variance to obtain a sparse co-
259 transcriptional network. Note that this model (**Figure 4A**, Model 3) is equivalent to Model 1 if
260 regularization is very stringent (all links between genes are dropped), and equivalent to Model 2 if no
261 regularization is applied (all links are present). By adjusting the level of regularization, we show that
262 temporal entropy can reach an accuracy of 1 (**Figure 4D**, Supplemental Figure 3D, E, Supplemental Table
263 5), demonstrating the utility of this single feature in classifying fitness outcomes.

264

265 The time course experiments accurately capture a bacterium’s survival in a test environment, but they are
266 labor intensive and potentially expensive. Therefore, a single time point prediction model was trained, by
267 quantifying the variance of the DE magnitude distribution for all single time points as a measure of entropy
268 (Supplementary Methods, Equation 1). Similar to the temporal models, the only parameter that we fit was

269 the threshold for entropy (in this case 2.07), which is the value that maximizes classification accuracy in
270 the training set. Analogous to the temporal models, low fitness is associated with higher entropy than high
271 fitness conditions (**Figure 4E**, Supplemental File 2). Importantly, cases of high and low fitness are better
272 separated at later time points (accuracy = 0.91 in the training and 0.92 in the test dataset) than at early
273 time points (accuracy = 0.74 in the training and 0.42 in the test dataset), indicating that time points from
274 the second half of the time course experiments are more characteristic of fitness outcome than those from
275 the first half (**Figure 4F**). Specifically, when applied on an independent test dataset, the single time point
276 entropy model led to 7 false positive predictions based on the early time points even though the
277 misclassified low fitness cases have a higher overall entropy than that of high fitness cases (**Figure 4G**).
278 This suggests that it is possible to successfully train an early time point-specific model if more training
279 data were used (Supplemental Figure 3A). In contrast, the single time point entropy predictor, with the
280 same threshold value of 2.07, performs very well for the late time points on the test dataset, misclassifying
281 only 1, that was very close to the threshold, out of 12 experiments (**Figure 4G**).
282

283 **Entropy-based fitness predictions are strain, species and stress-type independent and can be used
284 to infer the antibiotic minimum inhibitory concentration (MIC).**

285 To test if the entropy-based approach is generalizable and extends to other *S. pneumoniae* strains or other
286 species, a new RNA-Seq dataset was generated to predict fitness outcomes under ciprofloxacin exposure
287 for *Salmonella* Typhimurium, *S. aureus*, *E. coli*, *K. pneumoniae* and two additional *S. pneumoniae* strains
288 representing serotypes 1 and 23F (Supplemental Table 1). These five species represent both Gram-
289 negative and Gram-positive bacteria and cover a wide range of ciprofloxacin MICs (**Figure 5A**). The
290 overall response characteristics are similar to what was observed for *S. pneumoniae*, with 120 minutes
291 exposure to 1 μ g/mL ciprofloxacin triggering an expansion of expression changes from bacterial cultures
292 having low fitness (*S. Typhimurium* and *S. pneumoniae* serotype 1), compared to those with high fitness
293 (*S. pneumoniae* serotype 23F, *E. coli* and *K. pneumoniae*) (**Figure 5B**). When exposed to a higher dose
294 of CIP (strain-specific 1xMIC_{CIP}) the organisms with lower CIP-sensitivity were shown to trigger an
295 increased number of expression changes with a wider magnitude, indicative of their lowered fitness at the
296 increased concentration (**Figure 5B**, *S. pneumoniae* serotype 23F, *E. coli* and *K. pneumoniae*). Next, each
297 transcriptional response was captured by an entropy calculation. Importantly, with the original threshold
298 of 2.07 we had calibrated with data from *S. pneumoniae* in Figure 4, fitness outcomes could be predicted
299 for the new organisms with 100% accuracy, indicating that the amount of transcriptional disruption by

300 antibiotics is a species-independent generalizable feature for fitness outcome. Therefore, entropy could be
301 visualized graphically (**Figure 5B**), and quantified to make high-accuracy predictions.

302

303 Interestingly, the entropy measurement of each strain was found to be inversely proportional to the MIC_{CIP}
304 (**Figure 5C**), consistent with transcriptional disruption being proportional to stress sensitivity. The
305 correlation between entropy and ciprofloxacin sensitivity in **Figure 5C** (left panel) therefore implies that
306 the antibiotic sensitivity of any species could be predicted from its transcriptomic entropy. To test this,
307 entropy was calculated for *Acinetobacter baumannii* isolates that are either low (ATCC 17978) or high
308 (LAC-4) virulence, by collecting RNA-Seq profiles after 120 min exposure to 1 $\mu\text{g}/\text{mL}$ of ciprofloxacin.
309 Using a linear regression model, the ciprofloxacin MICs of the *A. baumannii* strains were predicted to be
310 0.04 and 10.45 $\mu\text{g}/\text{mL}$, which are proximate to the measured MIC's of 0.07 and 8.5 $\mu\text{g}/\text{mL}$ for ATCC 17978
311 and LAC-4, respectively (**Figure 5D**; Supplemental Figure 1D). This demonstrates that entropy can be
312 applied to determine antibiotic sensitivity for new species, and is not simply a binary indicator of fitness
313 outcomes.

314

315 To explore the applicability of entropy beyond nutrient and antibiotic stress, we performed entropy-based
316 fitness classification on a published collection of 193 *M. tuberculosis* transcription factor over-expression
317 (TFOE) strains (14). Upon TFOE, these strains exhibit fitness changes, ranging from severe growth
318 defects to small growth advantages (15). Over-expression of a single transcription factor can thereby exert
319 stress on the bacterium that can result in drastically different fitness outcomes. By calculating entropy
320 from whole-genome microarray data collected from each TFOE strain, using genome-wide DE under
321 inducing and noninducing conditions, it is possible to distinguish strains based on their fitness levels at an
322 accuracy of 0.78, using a newly trained entropy threshold for this dataset (**Figure 5E**). This result
323 compares favorably with a more complicated approach involving the integration of each TFOE
324 transcriptional profile into condition-specific metabolic models (14). These data show that entropy has the
325 potential to be utilized as a strong and generalizable fitness prediction method for both antibiotic and non-
326 antibiotic stress, using different data types and a large variety of bacterial strains and species.

327

328 **A systems-level view successfully predicts fitness and is less sensitive to noise from a single feature.**

329 While the transcriptome-based entropy-approach is a strong predictor of fitness, it is a relatively coarse
330 method as it captures only a single organizational level of the response; the transcriptome. In most

331 biological systems, changes occur across multiple levels, which are detected by alternative readouts, such
332 as identification of phenotypic changes resulting from mutations (16-21). Furthermore, entropy ignores
333 details present in the data, such as the type of stress and the functional roles of genes, that may increase
334 the accuracy or widen the applicability of the approach. For instance, within the transcriptomic data,
335 different gene sets show different levels of perturbation, as witnessed in *S. pneumoniae* T4, in which genes
336 in the category "Antibiotic Response and Sensing" show higher entropy than other functional categories
337 (**Figure 6A**, Supplemental Figure 4A). In contrast, essential genes are mainly down-regulated and
338 nonessential genes are evenly distributed as up- and down-regulated in the antibiotic challenge conditions
339 (**Figure 6B**, Supplemental Figure 4B).

340

341 In order to make use of these detailed observations, we assembled a set of 54 features that describe various
342 aspects of a response, the organism and the experienced stress. To this end, we considered the type of
343 stress, such as the MOA of an antibiotic, the phenotypic response to stress as characterized by Tn-Seq,
344 and the transcriptional response (**Figure 7A**; Supplemental File 3). This approach yields a large number
345 of features relative to the number of samples (54 features and 231 samples in the training set), so we
346 performed a round of feature selection using a regularized logistic regression model (**Figure 7A**). The six
347 most informative features (described in Supplemental Methods) were used to train an SVM that is able to
348 classify the fitness outcomes with high accuracy, by setting a threshold in which a probability >0.5
349 translates to high fitness, and probability <0.5 to low fitness (**Figure 7B**, Supplemental File 2,
350 Supplemental Figure 4C). Importantly, accurate predictions could be made at both early and late time
351 points for antibiotics that triggered a fast transcriptomic response, as low and high fitness outcomes were
352 well-separated as early as 20 min after rifampicin exposure and 30-45 min after vancomycin exposure
353 (**Figure 7B**). For other antibiotics, accurate predictions could only be made at later time points. For
354 example, kanamycin treatment resulted in false positives up to and including 120 min, possibly due to a
355 slow transcriptional response to this drug (**Figure 7B**; Supplemental Figure 2A, D, E -Kanamycin). The
356 primary advantage of this model is that it provides less ambiguous predictions compared to the predictive
357 models based solely on transcriptional entropy, with the prediction probability following a bimodal
358 distribution that has very few cases near the threshold ($= 0.5$) in the training or independently generated
359 test sets (**Figure 7C**). Furthermore, in the test set all misclassified cases are at the early (30 min) time
360 point, while 100% of the late time points (120 min) are classified correctly (**Figure 7D**). This classifier
361 (test set accuracy = 0.5 and 1 in early and late time points respectively) outperformed the single-time point

362 entropy classifier (test set accuracy = 0.42 and 0.92 in early and late time points respectively). Thus, by
363 increasing data resolution and including multiple data sources, a highly accurate model is achieved that is
364 robust to noise from a single data source.

365

366 **Discussion**

367 A major goal of this work was to determine if there is a quantifiable feature in the bacterial environmental
368 response that can accurately predict fitness in that environment that is independent of strain, species or
369 the type of stress. To be generalizable, the selected feature needs to be common across species and
370 environments. By generating a large experimental dataset we discovered that such a feature exists, namely
371 transcriptomic entropy, which represents the level of transcriptional disruption that occurs in a system
372 while responding to the environment. Centering on entropy, we develop a suite of statistical models that
373 vary in their complexity and that accommodate different types and amounts of input data enabling
374 predictions on the MOA of a stress, the fitness outcome of bacteria in a variety of different environments,
375 and the MIC.

376

377 The developed fitness prediction models differ in approach and input data required. The first model
378 extracts a small set of informative features from genome-wide transcriptional profiling data (i.e. a gene
379 panel). Although we have shown previously that phenotypic change and expression change rarely overlap
380 on the same genes, there are cases in which a gene can be simultaneously transcriptionally and
381 phenotypically important under a stressful condition (16). Indeed, several members of the fitness gene
382 panel are required for bacterial growth. For example, inhibition of the essential cell division gene *ftsZ* has
383 been shown to cause growth inhibition of MRSA (22). Among the non-essential genes, transposon
384 insertion mutants in SP_0929, SP_0589 and SP_1856 resulted in a significant fitness decrease in the
385 presence of multiple antibiotics (LVX, TET, CIP, CEF and RIF; Supplemental File 1). Therefore, further
386 characterization of the genes in this panel might reveal potential antimicrobial targets. Second, by applying
387 a first-principle approach, a single feature (entropy) is defined to capture an intuitive property of a
388 transcriptome: the extent of perturbation. Since entropy does not rely on responses in specific genes,
389 entropy-based models extend beyond a single species. Moreover, the single timepoint entropy can be used
390 in a regression model, offering a finer resolution by predicting the level of sensitivity to a particular stress
391 (in this case ciprofloxacin) as well. Finally, a third approach is a data-driven one, in which genome-wide
392 data across multiple biological systems were utilized (i.e. SVM for fitness prediction). Importantly, all
393 three types of fitness prediction models underscore that a bacterium's fitness phenotype is predictable,
394 and accurate predictions can be made in multiple pathogens independent of the mechanisms of stress,
395 including different classes of antibiotics and nutrient depletion.

396

397 By demonstrating the feasibility of predictions of fitness outcomes and antibiotic sensitivity, we believe
398 this work could provide novel opportunities to contribute to infectious disease diagnostics such as
399 antibiotic susceptibility testing (AST). Although AST can be completed in a relatively short amount of
400 time for many pathogenic species, it remains a lengthy process for slow-growing species such as *M.*
401 *tuberculosis* (23). Therefore, it is desirable to be able to predict the fitness outcome of such slow-growing
402 species as early as possible, for instance using RNA expression data. RNA-based detection has previously
403 been applied to correlate antibiotic susceptibility with the expression of several genes (5, 6, 24). However,
404 due to variability in gene-homology, such approaches can rapidly become species specific, and even when
405 a gene is present, the way it responds to a stress might not be the same. For instance, among the nine
406 strains and species we sampled here, the presence/absence of gene's in the 10-gene panel for fitness
407 predictions and their expression profiles are highly variable (Supplemental Figure 5A). Additionally, a
408 published *E. coli* ciprofloxacin sensitivity panel is highly specific for that species due to variability in
409 presence/absence and expression patterns (Supplemental Figure 5B; (5)). This indicates, that gene-panel
410 approaches may indeed quickly become strain, species and stress-type dependent. In contrast, we show
411 that entropy-based fitness predictions are independent of gene homology, which allows for
412 generalizability across different species under various stress-types (i.e. antibiotics, nutrient depletion and
413 transcription induction). Second, rather than being a binary prediction method, entropy can be applied to
414 predict the level of antibiotic sensitivity in a species-independent manner, which is useful to determine a
415 bacterium's level of susceptibility to an antibiotic without performing possibly more extensive growth-
416 based assays or identifying the resistance genes or mutations by whole-genome sequencing. Importantly,
417 we show that MIC predictions can be achieved by profiling the transcriptome of a bacterium at a single
418 time-point and a single concentration of an antibiotic, requiring little prior knowledge of antibiotic MOA
419 or direct targets in the tested species. Our entropy-based antibiotic sensitivity prediction could therefore
420 contribute to improving the speed and generalizability of existing AST methods.

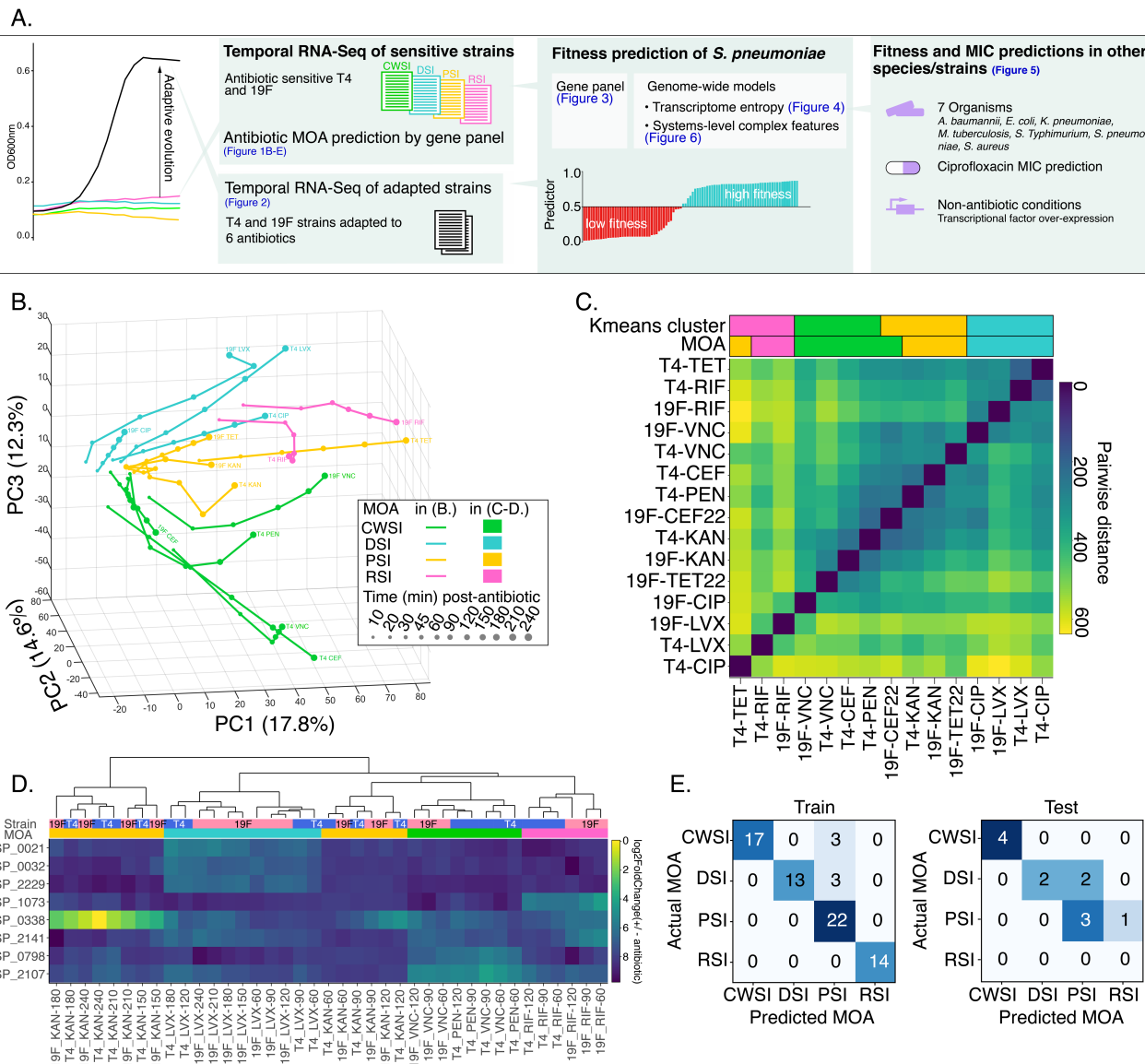
421
422 Since transcriptional entropy captures information at a single level, several improvements could be
423 implemented to potentially enhance the fitness prediction model. We show that some antibiotics trigger a
424 faster response while some trigger a slower response (Supplemental Figure 2A, D, E). Consequently, it
425 would make more sense to apply a fitness-predictor to the transcriptomic profile at a later timepoint for
426 antibiotics that trigger a slower response such as kanamycin; but an earlier timepoint can be used for
427 antibiotics such as rifampicin. Knowing (or predicting) the type of antibiotic being used can therefore

428 inform when to use a fitness predictor, i.e. fitness predictions can potentially be enhanced when the MOA
429 and fitness predictors are used in tandem. As indicated by the data-driven complex feature model, fitness
430 predictions are improved when fine-grained information on the bacterial stress response is included.
431 Additional types of data as well as the consideration of more features may thus improve fitness predictions
432 through the inclusion of more detailed information. Thus, by gathering and integrating information
433 pertaining to the host environment, for instance by simultaneous transcriptomic profiling via dual RNA-
434 Seq(25) and cytokine profiling of the host response, our model might be able to infer and monitor disease
435 progression *in vivo*.

436

437 To conclude, with entropy we present a novel concept that is independent of gene-identity, gene-function,
438 and type of stress, and can be applied as a fundamental building block for generalizable statistical models
439 that accurately predict bacterial fitness and MICs for Gram-positive and negative species alike.

440

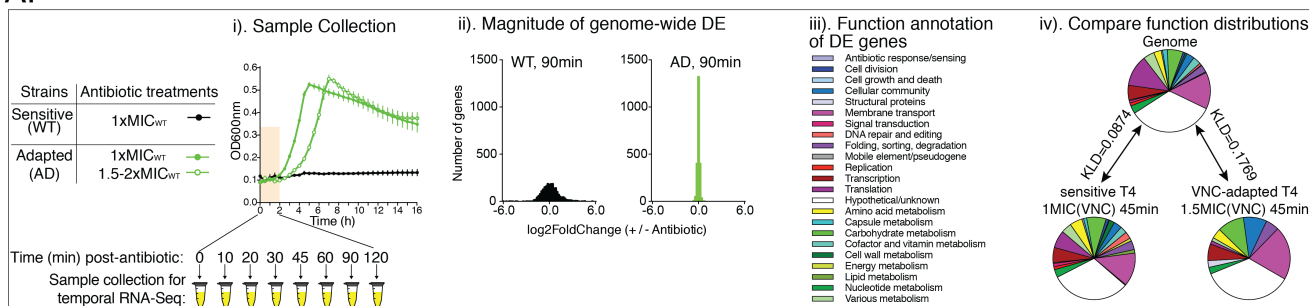


441

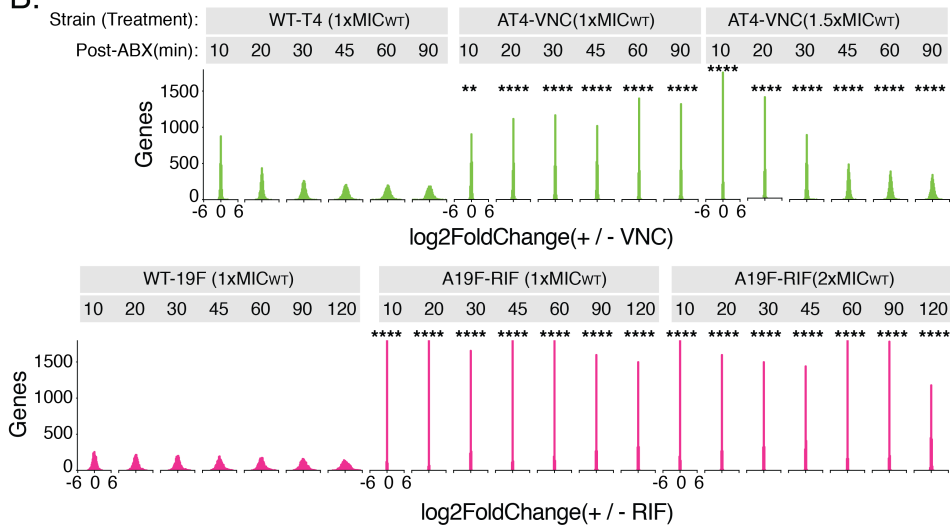
442 **Figure 1. Transcriptional responses separate antibiotics with different mechanisms of action (MOA's).**

443 **A.** Project setup and overview. Wildtype and adapted strains of *S. pneumoniae* were exposed to different classes of antibiotics, and their fitness outcomes were determined from growth curves. Temporal RNA-Seq data was used to train models that predict the MOA of an antibiotic, and the fitness outcome of a strain. The concept of entropy is developed expanding predictions on fitness to other strains and species and non-antibiotic conditions. CWSI (cell wall synthesis inhibitors): PEN – penicillin, VNC – vancomycin, CEF – cefepime; DSI (DNA synthesis inhibitors): CIP – ciprofloxacin, LVX – levofloxacin; RSI (RNA synthesis inhibitor): RIF – rifampicin; PSI (protein synthesis inhibitors): KAN – kanamycin. TET – tetracycline. **B.** Principal component analysis (PCA) of differential expression datasets (log2FoldChange of +/- antibiotic) from sensitive strains depicts antibiotic responses as largely distinct temporal transcriptional trajectories. **C.** Pairwise distances between PCA trajectories (see Supplementary Methods). Transcriptional trajectories to drugs within the same MOA are similar and tend to cluster together indicated by k-means clustering. **D.** Heatmap of differential expression of an 8-gene panel. Dendrogram shows antibiotic MOA's can be well separated by differential expression of this gene panel. **E.** Antibiotic MOA prediction by a support vector machine (SVM) trained on differential expression profiles of the 8-gene panel in a training set (Train) and test set (Test). Color intensity is proportional to the number of predictions.

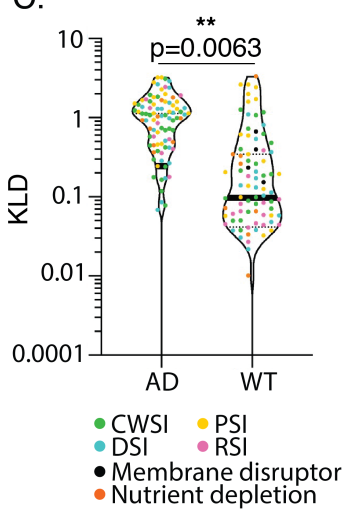
A.



B.



C.

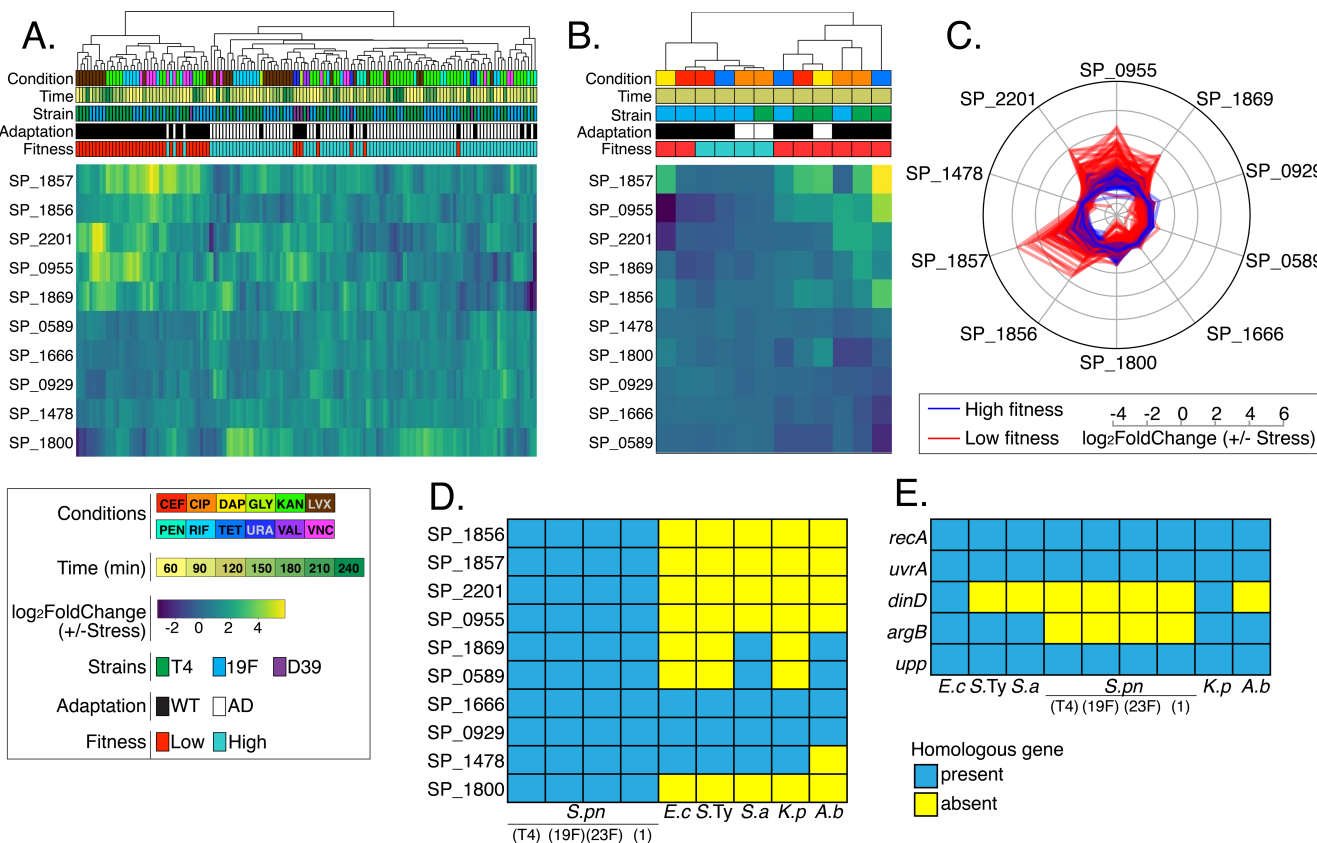


458

459 **Figure 2. A transcriptional response separates bacteria with different sensitivities to the same**
460 **antibiotic.**

461 A. A schematic illustration of temporal RNA-Seq sample collection (i) and data processing (ii-iv) on stress-sensitive
462 wild-type (WT) and stress-insensitive adapted strains (AD), which are obtained through experimental evolution of
463 the WT strains. Magnitude distribution of genome-wide differential expression is compared between each pair of
464 WT and AD strains (ii). Genes in the *S. pneumoniae* genomes are divided over 23 gene function categories (see
465 figure legend). Kullback-Leibler divergence (KLD) of gene function distributions between genes with significant
466 expression changes and function distribution of all genes present in the genome (iii). A similar function distribution
467 to the genome is indicated by a low KLD value, e.g. T4-VNC(1xMIC)-45min, while a dissimilar function
468 distribution is indicated by a high KLD value, e.g. VNC-adapted T4-VNC(1.5xMIC)-45min (iv).

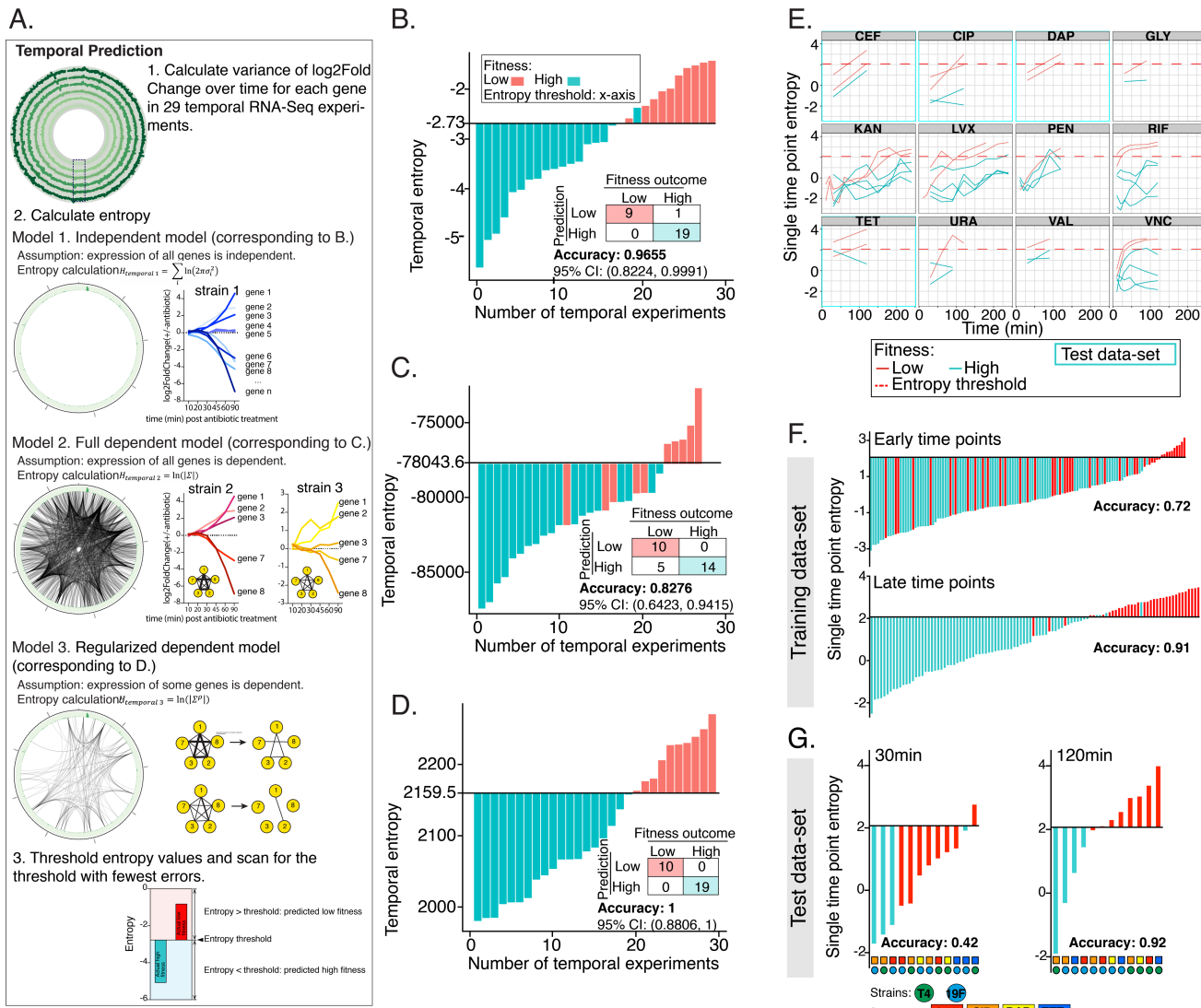
469 B. The magnitude of genome-wide differential expression (indicated as log2FoldChange Antibiotic/NDC (no drug
470 control)) shows significantly wider distributions in antibiotic-sensitive strains (wtTIGR4 and wt19F) compared to
471 antibiotic-adapted strains in the presence of vancomycin (a cell wall synthesis inhibitor; CWSI) and rifampicin (an
472 RNA synthesis inhibitor; RSI), respectively in a Kolmogorov-Smirnov test. *: 0.001 < p < 0.05; **: 0.0001 < p < 0.001;
473 ***: p < 0.0001. See **Supplemental Figure 2D, E** for other antibiotics. All histograms are on the same scale of -6 to
474 6. C. AD have a significantly higher KLD than WT in the presence of antibiotics or absence of D39-essential
475 nutrients in an unpaired t-test.



476
477
478

Figure 3. A 10-gene panel predicts fitness outcomes of *S. pneumoniae* under antibiotic and nutrient stress.

479 A 10-gene panel is generated by logistic regression on 231 RNA-Seq profiles collected from antibiotic exposure or
480 D39-essential nutrient depletion conditions in stress-sensitive and stress-insensitive strains. Log₂fold change (+/-
481 stress) of the 10-gene panel for fitness is indicated by the heat-map color gradients, which separates high fitness
482 (blue in the 'Fitness' bar) from low fitness (red) in a training (A.) and test set (B.). C. Differential expression of
483 each gene in the gene panel is depicted as a radar plot, showing a clear difference between low (red) and high (blue)
484 fitness outcomes. Presence and absence of each gene in the *S. pneumoniae* fitness panel (D.) or *E. coli* ciprofloxacin
485 sensitivity panel (E; (5)) in six pathogenic species is first determined by protein BLAST based on three criteria:
486 query coverage > 50%, E value < 1E-50 and percent identity > 30%, indicating that genes in a gene panel are poorly
487 conserved and thus might suffer a limited generalizability across multiple species. *S.pn*: *S. pneumoniae*, *E.c*: *E. coli*,
488 *S.Ty*: *S. Typhimurium*, *S.a*: *S. aureus*, *K.p*: *K. pneumoniae*, *A.b*: *A. baumannii*



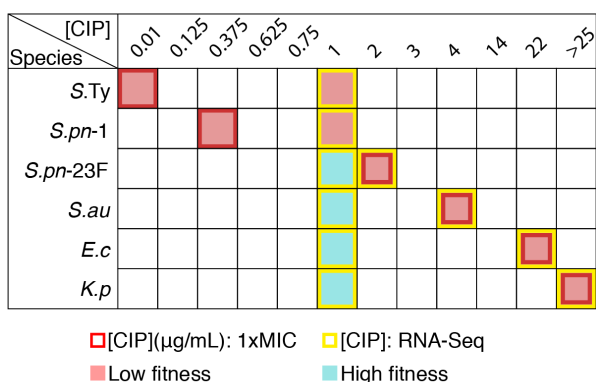
489

490 **Figure 4. Temporal and single time point entropy calculated from a transcriptional response**
 491 **predicts high and low fitness outcomes.**

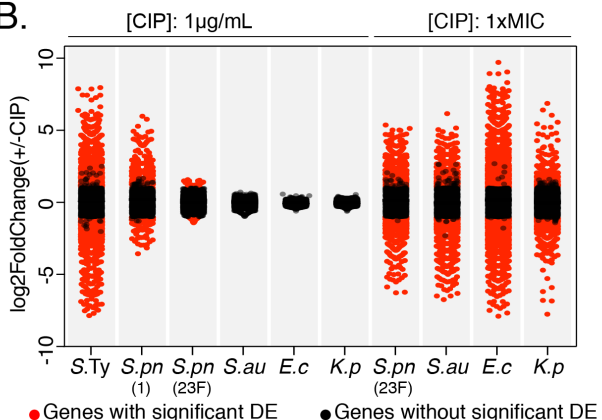
492 A. Illustration of the three temporal entropy models (Models 1-3) that are applied on 29 temporal RNA-Seq
 493 experiments. B.-D. Temporal fitness prediction is shown as a ranked plot of entropy in each temporal RNA-Seq
 494 dataset. The y-intercept indicates the entropy threshold, i.e. entropy higher than threshold is predicted as a low
 495 fitness outcome; entropy lower than threshold is predicted as a high fitness outcome. A confusion matrix is
 496 generated for each model by comparing to the actual fitness outcome (High/low fitness: cyan/red bars). E. Single
 497 time point entropy is calculated from differential expression of all genes in an experiment at one time point and
 498 plotted against time post-stress exposure (presence of antibiotics – CEF, CIP, DAP, KAN, LVX, PEN, RIF, TET,
 499 VNC, or absence of nutrients – Glycine-GLY, Uracil-URA, Valine-VAL). Dashed red line indicates the entropy
 500 threshold for this model. Training and test sets are indicated by grey or blue borders respectively. Fitness prediction
 501 is performed at each single time point (231 data points) in the 29 temporal experiments as the training set (F.), and
 502 validated by an independent set of single time point RNA-Seq experiments as the test set (24 data points; G.). In
 503 both training (F.) and test (G.) datasets, fitness prediction is more accurate from late time points than early time
 504 points indicating late time points are more characteristic of a strain's fitness outcome.

505

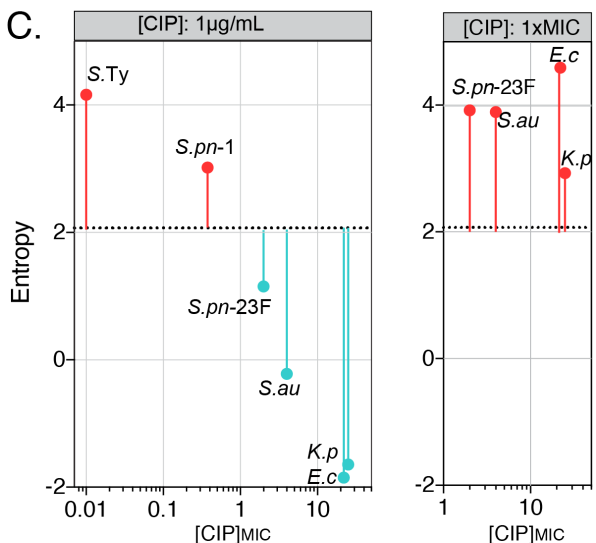
A.



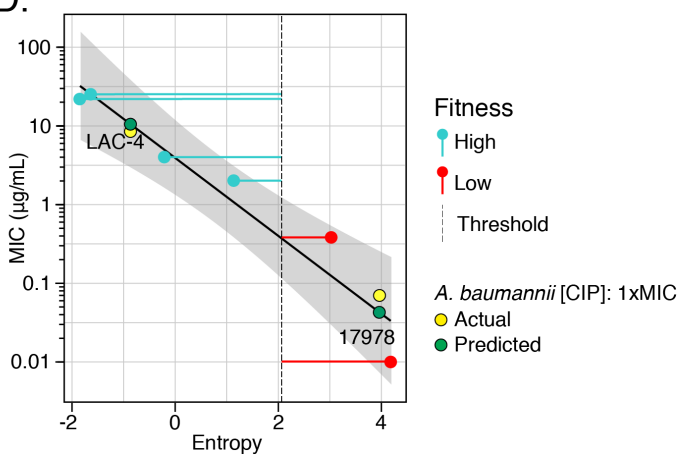
B.



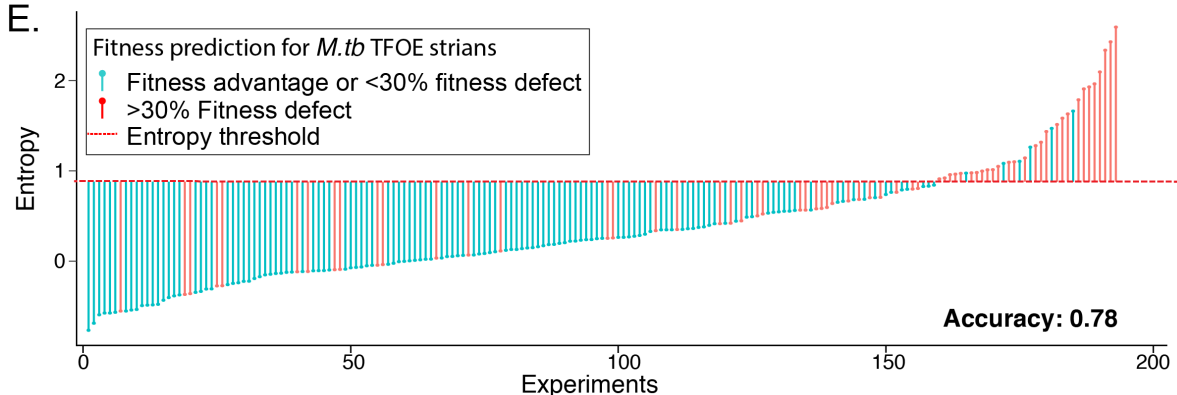
C.



D.



E.



506

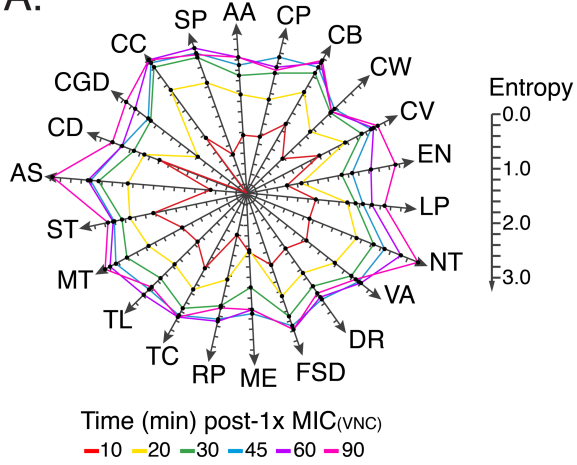
507 **Figure 5. Entropy based fitness predictions extend to multiple species under antibiotic and non-**
508 **antibiotic stress.**

509 A. Six strains representing 5 species are ranked from low to high ciprofloxacin minimal inhibitory concentrations
510 (MIC_{CIP}) tested by growth curve assays. The multi-species CIP RNA-Seq is performed at two CIP concentrations:
511 1) 1 μg/mL for all 6 strains corresponding to 2 low fitness outcomes (red squares) and 4 high fitness outcomes (cyan
512 squares); 2) MIC_{CIP} for strains that are insensitive to 1 μg/mL of CIP, i.e. *S. pneumoniae* serotype 23F, *S. aureus*
513 UCSD Mn6, *E. coli* AR538, and *K. pneumoniae* AR497, corresponding to 4 additional low fitness outcomes.

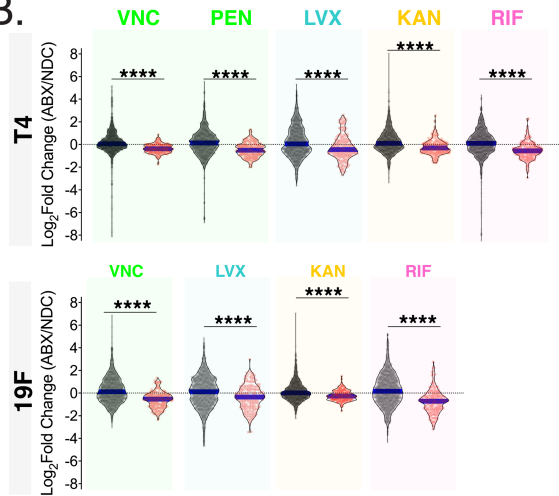
514 The number of genes that change in expression upon exposure to 1 μg/mL CIP (|log2FoldChange| > 1 and p-adj < 0.05)

515 as well as their change in magnitude is inversely correlated to their CIP sensitivity (**B.**) and their entropy (**C.**).
516 Additionally, strains with MIC_{CIP} higher than 1 $\mu\text{g}/\text{mL}$ revert to triggering a large number of differential expression
517 genes (**B.**) and a high entropy (**C.**) at their respective 1 $\times\text{MIC}_{\text{CIP}}$.
518 **D.** Using a linear regression model (black line; error band: 95% CI), MIC's are predicted for *A. baumannii* strains
519 ATCC 17978 and LAC-4 based on their entropy at 1 $\mu\text{g}/\text{mL}$ of ciprofloxacin. The predicted (black) and measured
520 (red) MIC for the two strains are similar for both strains. See **Supplemental Figure 1D** for MIC determination for
521 *A. baumannii* ATCC17978 and LAC-4.
522 **E.** Entropy calculated from transcriptional profiles of 193 *M. tuberculosis* transcription factor over-expression
523 (TFOE) strains separates strains with a >30% fitness defect upon TFOE induction (red) from strains with a fitness
524 advantage or <30% fitness defect upon induction (cyan). At the threshold of 0.71 (red dotted line), fitness outcomes
525 are correctly predicted at an accuracy of 0.78.

A.



B.



526

527

528

529

530

531

532

533

534

535

536

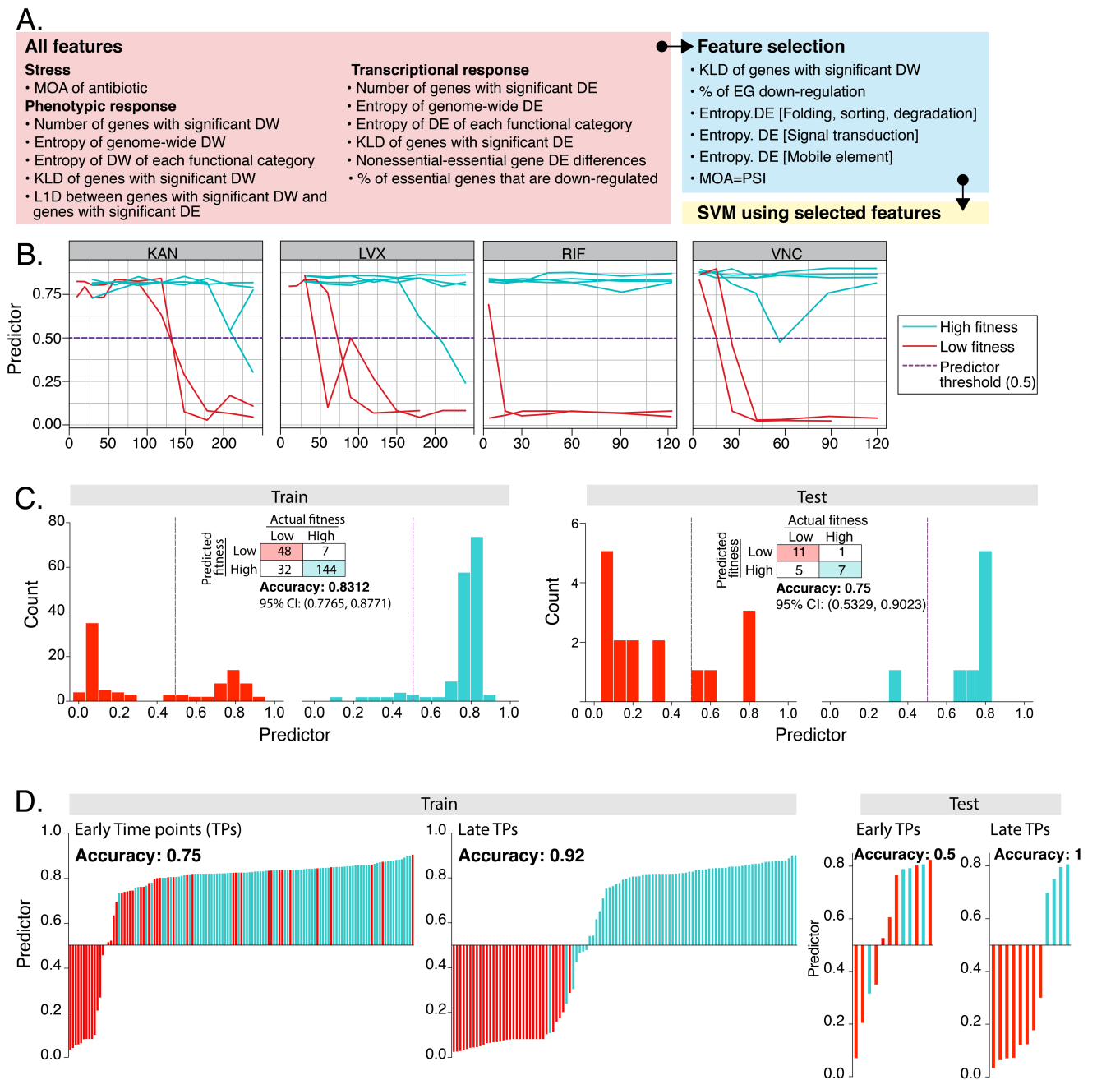
537

538

539

Figure 6. Detailed features can be extracted from transcriptomic responses of strains with low and high fitness outcomes.

A. The entropy of a transcriptional response can be split by gene function to indicate the level of transcriptional perturbation in each cellular system. AA: amino acid metabolism, CP: capsule metabolism, CB: carbohydrate metabolism, CW: cell wall metabolism, CV: cofactors and vitamin metabolism, EN: energy metabolism, LP: lipid metabolism, NT: nucleotide metabolism, VA: various metabolism, DR: DNA repair, FSD: folding, sorting and degradation, ME: mobile elements. RP: replication, TC: transcription, TL: translation, MT: membrane transport, ST: signal transduction, AS: antibiotic sensing, CD: cell division, CGD: cell growth and death, CC: cellular community, SP: structural proteins. B. Essential genes tend to be significantly more down-regulated compared to non-essential genes in stress-sensitive strains (wt-T4; unpaired t-test, *: 0.001<p<0.05; **: 0.0001<p<0.001; ***: p<0.0001).



540

541

Figure 7. A systems-level view of the bacterium further improves fitness predictions.

542 A. Illustration of the construction of a complex feature classifier (CFC) in three main steps: 1) assembly of all input
543 features, 2) feature selection and 3) SVM-based fitness predictions.

544 B. Prediction probabilities generated by the CFC are plotted at each time point for strains with high fitness (cyan line)
545 and low fitness (red line) in the presence of KAN, LVX, RIF, and VNC. A probability higher than the threshold
546 (0.50; red dotted line) is predicted as high fitness; while a predictor lower than the threshold is predicted as low
547 fitness.

548 C. Performance of the CFC on training and test datasets is shown as frequency distributions of prediction
549 probabilities separated by actual fitness outcomes and the corresponding confusion matrices.

550 D. High (cyan) and low (red) fitness outcomes are mostly well separated by the CFC predictor at the threshold of
551 0.50. Similar to the single time point entropy model (Figure 3), fitness prediction by the CFC achieves a much
552 higher accuracy of 1.0 at late time points compared to early time points.

553

554 **References**

- 556 1. Chatterjee A, Saranath D, Bhatter P, & Mistry N (2013) Global transcriptional profiling of longitudinal
557 clinical isolates of *Mycobacterium tuberculosis* exhibiting rapid accumulation of drug resistance. *PLoS*
558 *One* 8(1):e54717.
- 559 2. Erill I, Campoy S, & Barbe J (2007) Aeons of distress: an evolutionary perspective on the bacterial SOS
560 response. *FEMS Microbiol Rev* 31(6):637-656.
- 561 3. Little JW & Mount DW (1982) The SOS regulatory system of *Escherichia coli*. *Cell* 29(1):11-22.
- 562 4. Yim G, McClure J, Surette MG, & Davies JE (2011) Modulation of *Salmonella* gene expression by
563 subinhibitory concentrations of quinolones. *J Antibiot (Tokyo)* 64(1):73-78.
- 564 5. Barczak AK, *et al.* (2012) RNA signatures allow rapid identification of pathogens and antibiotic
565 susceptibilities. *Proc Natl Acad Sci U S A* 109(16):6217-6222.
- 566 6. Suzuki S, Horinouchi T, & Furusawa C (2014) Prediction of antibiotic resistance by gene expression
567 profiles. *Nat Commun* 5:5792.
- 568 7. Horinouchi T, *et al.* (2017) Prediction of Cross-resistance and Collateral Sensitivity by Gene Expression
569 profiles and Genomic Mutations. *Sci Rep* 7(1):14009.
- 570 8. Boutte CC & Crosson S (2013) Bacterial lifestyle shapes stringent response activation. *Trends Microbiol*
571 21(4):174-180.
- 572 9. Baharoglu Z & Mazel D (2014) SOS, the formidable strategy of bacteria against aggressions. *FEMS*
573 *Microbiol Rev* 38(6):1126-1145.
- 574 10. Ling J, *et al.* (2012) Protein aggregation caused by aminoglycoside action is prevented by a hydrogen
575 peroxide scavenger. *Mol Cell* 48(5):713-722.
- 576 11. Lin JT, Connelly MB, Amolo C, Otani S, & Yaver DS (2005) Global transcriptional response of *Bacillus*
577 *subtilis* to treatment with subinhibitory concentrations of antibiotics that inhibit protein synthesis.
578 *Antimicrob Agents Chemother* 49(5):1915-1926.
- 579 12. Mascher T, Heintz M, Zahner D, Merai M, & Hakenbeck R (2006) The CiaRH system of *Streptococcus*
580 *pneumoniae* prevents lysis during stress induced by treatment with cell wall inhibitors and by mutations
581 in *ppb2x* involved in beta-lactam resistance. *J Bacteriol* 188(5):1959-1968.
- 582 13. Schweizer I, *et al.* (2017) New Aspects of the Interplay between Penicillin Binding Proteins, *murM*, and
583 the Two-Component System CiaRH of Penicillin-Resistant *Streptococcus pneumoniae* Serotype 19A
584 Isolates from Hungary. *Antimicrob Agents Chemother* 61(7).
- 585 14. Rustad TR, *et al.* (2014) Mapping and manipulating the *Mycobacterium tuberculosis* transcriptome using
586 a transcription factor overexpression-derived regulatory network. *Genome Biol* 15(11):502.
- 587 15. Ma SM, R.; Hobbs, S. J.; Farrow-Johnson, J.; Rustad, T. R.; Sherman, D. R. (2018) Network stress test
588 reveals novel drug potentiators in *Mycobacterium tuberculosis*. *bioRxiv* 429373.
- 589 16. Jensen PA, Zhu Z, & van Opijnen T (2017) Antibiotics Disrupt Coordination between Transcriptional and
590 Phenotypic Stress Responses in Pathogenic Bacteria. *Cell Rep* 20(7):1705-1716.
- 591 17. van Opijnen T, Bodi KL, & Camilli A (2009) Tn-seq: high-throughput parallel sequencing for fitness and
592 genetic interaction studies in microorganisms. *Nat Methods* 6(10):767-772.
- 593 18. van Opijnen T & Camilli A (2013) Transposon insertion sequencing: a new tool for systems-level
594 analysis of microorganisms. *Nat Rev Microbiol* 11(7):435-442.
- 595 19. van Opijnen T & Camilli A (2012) A fine scale phenotype-genotype virulence map of a bacterial
596 pathogen. *Genome Res* 22(12):2541-2551.
- 597 20. van Opijnen T & Camilli A (2010) Genome-wide fitness and genetic interactions determined by Tn-seq, a
598 high-throughput massively parallel sequencing method for microorganisms. *Curr Protoc Microbiol*
599 Chapter 1:Unit1E 3.
- 600 21. van Opijnen T, Dedrick S, & Bento J (2016) Strain Dependent Genetic Networks for Antibiotic-
601 Sensitivity in a Bacterial Pathogen with a Large Pan-Genome. *PLoS Pathog* 12(9):e1005869.
- 602 22. Liang S, *et al.* (2015) Inhibiting the growth of methicillin-resistant *Staphylococcus aureus* in vitro with
603 antisense peptide nucleic acid conjugates targeting the *ftsZ* gene. *Int J Infect Dis* 30:1-6.

604 23. Jenkins SG & Schuetz AN (2012) Current concepts in laboratory testing to guide antimicrobial therapy.
605 *Mayo Clin Proc* 87(3):290-308.

606 24. Cornforth DM, *et al.* (2018) *Pseudomonas aeruginosa* transcriptome during human infection. *Proc Natl*
607 *Acad Sci U S A* 115(22):E5125-E5134.

608 25. Aprianto R, Slager J, Holsappel S, & Veening JW (2016) Time-resolved dual RNA-seq reveals extensive
609 rewiring of lung epithelial and pneumococcal transcriptomes during early infection. *Genome Biol*
610 17(1):198.

611